

# Oxidative Esterification of Aldehydes to Esters over Anchored Phosphotungstates

Sukriti Singh · Anjali Patel

Received: 5 May 2014 / Accepted: 17 June 2014 / Published online: 16 July 2014  
© Springer Science+Business Media New York 2014

**Abstract** 12-Tungstophosphoric acid and lacunary phosphotungstate anchored to MCM-41 and  $\text{ZrO}_2$  were synthesized, characterized and used as bifunctional catalyst for oxidative esterification of benzaldehyde with methanol. The different aldehyde substrates study show excellent selectivity for esters, indicating the scope of the catalysts. A tentative reaction mechanism for oxidative esterification of aldehyde is also proposed.

**Keywords** Phosphotungstates · Anchored · Oxidative esterification · Aldehydes · Esters

## 1 Introduction

Methyl esters are traditionally prepared by the reaction of carboxylic acid and methanol using acid catalysts such as sulfuric, sulfonic, phosphoric, hydrochloric and *p*-toluenesulfonic acid [1, 2]. Alkoxides, such as sodium and potassium alkoxides, have also been used to prepare methyl esters from carboxylic acid precursors [3]. However, the direct oxidative esterification of aldehyde, avoiding the use of the corresponding carboxylic acid, is very attractive. This reaction typically takes place in a two-step procedure, first the oxidation of the aldehyde with manganese dioxide or sodium dichromate, and the subsequent conversion of the carboxylic acid intermediate to methyl ester.

Hence, oxidative esterification of aldehydes [4] has received increasing attention during recent years, as it

allows oxidation as well as esterification in one pot. One-step conventional methods reported require the use of heavy-metal oxidants such as  $\text{KMnO}_4$  [5],  $\text{CrO}_3$  [6], oxone [7],  $\text{V}_2\text{O}_5$ -SPC/SPB (SPC-sodium percarbonate, SPB sodium perborate) [8] and 1,5-cyclooctadiene (cod) complex of Iridium i.e.  $[\text{IrCl}(\text{cod})]_2/\text{K}_2\text{CO}_3$  [9]. Most of the reported methods are useful for direct transformation of aldehydes with alcohols to corresponding esters. However, many methods suffer from disadvantages such as use of expensive and polluting reagents, an inert atmosphere and lengthy reaction times. Due to the huge amount of toxic wastes and by-products arising from chemical processes, chemists have been constrained to develop cost-effective and environmentally friendly catalytic routes that minimize waste.

Recently, various groups have reported oxidative esterification of aldehydes based on supported Gold-Nickel Oxide ( $\text{AuNiOx}$ ) [10], TS-1 [11], supported gold nanoparticle  $\text{Au}/\text{TiO}_2$  [12], Pb and Mg doping in  $\text{Al}_2\text{O}_3$ -supported Pd [13], ionic liquid  $\text{BmimBF}_4$  [14], manganese phthalocyanine immobilized on silica gel [15]. Consequently from the viewpoint of demands as well as significance of acid and oxidation reactions, it would be more beneficial if a bifunctional catalyst could be developed for oxidative esterification of aldehydes.

Catalysis by supported phosphotungstates [16, 17] have greatly expanded during the last few years from the view point of their variety in structures and compositions. It is one of the most successful areas in contemporary catalysis, where systematic studies of phosphotungstate catalysts at the molecular level have led to a string of large-scale industrial applications [18, 19]. The acidic as well as redox properties are a function of the nature of the metal atoms (addenda atoms) and of both the heteroatom and the counter ions [20–25]. The replacement of one or more

S. Singh · A. Patel (✉)  
Polyoxometalates and Catalysis Laboratory, Department of  
Chemistry, Faculty of Science, The M.S. University of Baroda,  
Vadodra 390002, India  
e-mail: aupatel\_chem@yahoo.com

addenda atoms is expected to tune the acidic as well as redox properties. These active species are called as lacunary phosphotungstates ( $\text{PW}_{11}\text{O}_{39}$ )<sup>7-</sup> [26–28].

Our group has been working in the field of supported parent [29, 30] and lacunary phosphotungstates [31–33] and has successfully established the use of these materials for various organic transformations comprising of acid catalyzed as well as oxidation reactions. Recently we have reported bifunctional catalytic activity of 12-tungstophosphoric acid supported on metal oxide as well as mesoporous material for esterification and oxidation of benzyl alcohol [34]. We have also successfully evaluated the bifunctional catalytic activity of lacunary phosphotungstates for esterification as well as oxidation reactions [33]. Due to the encouraging results of these reactions and also because of the known industrial importance of esters as well as carbonyl compounds, as an extension of our work, it was thought of interest to evaluate the use of these materials as bifunctional catalysts for oxidative esterification reaction, where oxidation and esterification take place in one pot.

As per our knowledge only two reports are available on oxidative esterification of aldehydes with  $\text{H}_2\text{O}_2$  using 12-tungstophosphoric acid. One is 12-tungstophosphoric acid immobilized on the surface of silica encapsulated  $\gamma\text{-Fe}_2\text{O}_3$  nanoparticles [35] and the other being imidazolium polyoxometalate [bmim]<sub>3</sub>[ $\text{PW}_{12}\text{O}_{40}$ ] [36].

In the present work, different catalysts based on parent phosphotungstate ( $\text{H}_3\text{PW}_{12}\text{O}_{40}$ ) and lacunary phosphotungstate ( $\text{PW}_{11}\text{O}_{39}$ )<sup>7-</sup> anchored to MCM-41 and Zirconia were synthesised and characterized. Consequently the effect of various reaction parameters such as mole ratio, catalyst amount, time, and temperature were studied to optimize the conditions for maximum conversion by taking benzaldehyde as model substrate for the reaction. The versatility of using  $\text{H}_2\text{O}_2$  as an efficient oxidant in the transformation of benzaldehyde to methyl benzoate was also studied. The work was extended by carrying out oxidation of different aldehyde substrates. The main part of the research highlights the possibility of catalyst recycling. Effort was made to systematically evaluate the role of supports and catalysts in the reaction as well as propose a suitable mechanism. The final goal of the present paper is therefore to obtain an active, selective and recyclable catalytic system.

## 2 Method

### 2.1 Materials

All chemicals used were of A.R. grade. 12-tungstophosphoric acid ( $\text{PW}_{12}$ ),  $\text{ZrOCl}_2 \cdot 8\text{H}_2\text{O}$  (Zirconium oxychloride), ammonia, Cetyltrimethyl ammonium bromide

(CTAB), TEOS (tetraethyl orthosilicate), Sodium tungstate dihydrate, anhydrous disodium hydrogen phosphate, acetone, nitric acid, aldehydes, methanol were used as received from Merck.

### 2.2 Synthesis of $\text{PW}_{11}$ and the Supports

The sodium salt of  $\text{PW}_{11}$  was successfully synthesized and characterized by the same method reported by us [31]. Sodium tungstate dihydrate (0.22 mol, 72.5 g) and anhydrous disodium hydrogen phosphate (0.02 mol, 2.84 g) were dissolved in 150–200 mL of double distilled water and heated to 80–90 °C followed by the addition of concentrated nitric acid in order to adjust the pH to 4.8. The volume was then reduced to half by evaporation and the heteropoly anion was separated by liquid–liquid extraction with 80–100 mL of acetone. The extraction was repeated until the acetone extract showed absence of nitrate ions. The extracted sodium salt was dried in air.

MCM-41 was synthesized by following procedure reported by us [37]. Surfactant (CTAB) was added to the very dilute solution of NaOH with stirring at 60 °C. When the solution became homogeneous, TEOS was added drop wise, and the obtained gel was aged for 2 h. The resulting product was filtered, washed with distilled water, and then dried at room temperature. The obtained material was calcined at 550 °C in air for 5 h and designated as MCM-41.

Hydrous zirconia was prepared by following method reported by [38]. Aqueous ammonia solution was added to aqueous solution of  $\text{ZrOCl}_2 \cdot 8\text{H}_2\text{O}$  upto pH 8.5. The precipitates were aged at 100 °C over a water bath for 1 h, filtered, washed with conductivity water until chloride free water was obtained and dried at 100 °C for 10 h. The obtained material is designated as  $\text{ZrO}_2$ .

### 2.3 Synthesis of the Catalysts

A series of catalysts containing 10–40 % of  $\text{PW}_{12}$  anchored to MCM-41 and Zirconia were synthesized by impregnating an aqueous solution of  $\text{PW}_{12}$  (0.1/10–0.4/40  $\text{gmL}^{-1}$  of double distilled water) with MCM-41 (1 g) and dried at 100 °C for 10 h. The obtained materials were designated as ( $\text{PW}_{12}$ )<sub>1</sub>/MCM-41, ( $\text{PW}_{12}$ )<sub>2</sub>/MCM-41, ( $\text{PW}_{12}$ )<sub>3</sub>/MCM-41, and ( $\text{PW}_{12}$ )<sub>4</sub>/MCM-41, respectively. A series of catalysts containing 10–40 % of  $\text{PW}_{12}$  supported on  $\text{ZrO}_2$  was synthesized following the same method and the resulting materials were designated as ( $\text{PW}_{12}$ )<sub>1</sub>/ $\text{ZrO}_2$ , ( $\text{PW}_{12}$ )<sub>2</sub>/ $\text{ZrO}_2$ , ( $\text{PW}_{12}$ )<sub>3</sub>/ $\text{ZrO}_2$ , and ( $\text{PW}_{12}$ )<sub>4</sub>/ $\text{ZrO}_2$ , respectively.

Catalyst was synthesized by impregnating pure MCM-41 (1 g) with an aqueous solution of  $\text{PW}_{11}$  (0.1–0.4 g in 10–40 mL of double distilled water) and dried at 100 °C for 10 h. The obtained materials were treated with 0.1 N

HCl, filtered, washed with double distilled water and dried at 100 °C. The obtained materials were designated as (PW<sub>11</sub>)<sub>1</sub>/MCM-41, (PW<sub>11</sub>)<sub>2</sub>/MCM-41, (PW<sub>11</sub>)<sub>3</sub>/MCM-41, (PW<sub>11</sub>)<sub>4</sub>/MCM-41. A series of catalysts containing 10–40 % of PW<sub>11</sub> supported on ZrO<sub>2</sub> was synthesized following the same method. The obtained materials were designated as (PW<sub>11</sub>)<sub>1</sub>/ZrO<sub>2</sub>, (PW<sub>11</sub>)<sub>2</sub>/ZrO<sub>2</sub>, (PW<sub>11</sub>)<sub>3</sub>/ZrO<sub>2</sub>, and (PW<sub>11</sub>)<sub>4</sub>/ZrO<sub>2</sub>, respectively.

## 2.4 Characterization

A detailed study on the characterizations of all the synthesized catalysts can be found in our earlier publications [31, 37, 38]. However in the present article FT-IR, BET, total acidity measurements, FT-Raman, and XRD are given for reader's convenience.

FT-IR spectra were obtained by using the KBr wafer on the Perkin Elmer instrument. Adsorption–desorption isotherms of samples were recorded on a Micromeritics ASAP 2010 surface area analyzer at –196 °C. From adsorption–desorption isotherms surface area was calculated using the BET method. FT-Raman spectra were recorded on spectrophotometer Model Bruker FRA 106. The XRD pattern was obtained by using PHILIPS PW-1830. The conditions used were as follows: Cu K $\alpha$  radiation (1.5417 Å), scanning angle (2 $\theta$ ) from 0° to 60°. The total surface acidity was determined by *n*-butylamine titration [39]. A 0.025 M solution of *n*-butylamine in toluene was used for estimation. A 0.5 g catalyst mass was suspended in this solution for 24 h and excess base was titrated against trichloroacetic acid using neutral red as an indicator. This gives the total acidity of the material.

## 2.5 Catalytic Reaction

The reaction of benzaldehyde (0.01 mol) with H<sub>2</sub>O<sub>2</sub> (0.03 mol) and methanol was carried out in a 100 mL batch reactor provided with a double walled air condenser, Dean-Stark apparatus, magnetic stirrer, and a guard tube. The reaction mixture was refluxed at 80 °C for 6 h. The product was extracted with dichloromethane by repeated extractions. The obtained products were analyzed on a gas chromatograph (Shimatzu-2014) using a capillary column (RTX-5). The obtained products were identified by comparison with the authentic samples and finally by gas chromatography mass spectroscopy.

# 3 Results and Discussion

## 3.1 Catalyst Characterization

The typical FT-IR bands for PW<sub>12</sub> are seen at 1080, 987, 893 and 800 cm<sup>-1</sup> corresponding to P–O, W=O and W–O–W

stretching, respectively. The FT-IR spectrum of MCM-41 shows a broad band around 1,300–1,000 cm<sup>-1</sup> corresponding to asymmetric stretching of Si–O–Si. The band at 801 and 458 cm<sup>-1</sup> are due to symmetric stretching and bending vibration of Si–O–Si, respectively. The band at 966 cm<sup>-1</sup> corresponds to symmetric stretching vibration of Si–OH. FT-IR spectra of (PW<sub>12</sub>)<sub>3</sub>/MCM-41 is almost same as that of MCM-41. The absence of respective FT-IR bands for PW<sub>12</sub> in (PW<sub>12</sub>)<sub>3</sub>/MCM-41 may be due to the overlapping of PW<sub>12</sub> bands with that of support. (PW<sub>12</sub>)<sub>3</sub>/ZrO<sub>2</sub> shows bands at 812, 964 and 1,070 cm<sup>-1</sup> corresponding to the symmetric stretching of W–O–W, W=O and P–O, respectively, indicating the retainment of the Keggin unit even after supporting on ZrO<sub>2</sub> [38].

The formation of lacunary PW<sub>11</sub> can be confirmed by splitting of P–O bond. The P–O stretching band (1,080 cm<sup>-1</sup>) for PW<sub>12</sub> splits into two new bands 1,085 and 1,043 cm<sup>-1</sup> in PW<sub>11</sub>. This is due to the loss of one W–O unit and lowering of the symmetry from Td (PW<sub>12</sub>) to Cs (PW<sub>11</sub>) around the central heteroatom, phosphorus [40]. The W–O–W and W=O stretching bands for PW<sub>11</sub> appear at 808, 863 and 952 cm<sup>-1</sup> respectively. The reported bands for PW<sub>11</sub>, at 1,085, 1043, 808 cm<sup>-1</sup> corresponding to P–O, W–O–W, respectively, are absent in (PW<sub>11</sub>)<sub>3</sub>/MCM-41 due to overlapping with the bands of MCM-41. But bands of PW<sub>11</sub> at 952 and 863 cm<sup>-1</sup> attributed to W=O and W–O–W, respectively shifts to a higher wave number (962 and 896 cm<sup>-1</sup>) in (PW<sub>11</sub>)<sub>3</sub>/MCM-41, indicating a strong interaction between the Keggin unit and the silanol group of support. The FT-IR spectrum of (PW<sub>11</sub>)<sub>3</sub>/ZrO<sub>2</sub> shows bands at 870, 958, 1097 and 1048 cm<sup>-1</sup> corresponding to the symmetric stretching of W–O–W, W=O and P–O bonds respectively. The positions are in good agreement with those of PW<sub>11</sub> confirming the presence of these groups in the synthesized materials.

The data for surface area and total acidity are presented in Table 1. The surface area decreases for catalysts as compared to the supports, except for (PW<sub>11</sub>)<sub>3</sub>/ZrO<sub>2</sub>. In case of (PW<sub>11</sub>)<sub>3</sub>/ZrO<sub>2</sub> the size of the active species (PW<sub>11</sub>) is smaller as compared to that of PW<sub>12</sub>. The small size may lead to close packing of particles and strong interaction with the support surface. This forms a surface overlayer that reduces the surface diffusion of zirconia and inhibits sintering, which results an increase in surface area. The decrease in surface area is the first evidence of chemical interaction of PW<sub>12</sub>/PW<sub>11</sub> with the supports. *N*-Butyl amine acidity values indicate that MCM-41 is fairly acidic as compared to ZrO<sub>2</sub> (Table 1). Acidity of all the catalysts increases as compared to the supports which is as expected.

Raman spectra of PW<sub>12</sub>, (PW<sub>12</sub>)<sub>3</sub>/MCM-41 and (PW<sub>12</sub>)<sub>3</sub>/ZrO<sub>2</sub> are shown in Fig. 1. The Raman spectrum of PW<sub>12</sub> shows bands at 1010, 990, 900, 550, and 217 cm<sup>-1</sup>, which are assigned to  $\nu_s$  (W–O<sub>d</sub>),  $\nu_{as}$  (W–O<sub>d</sub>),  $\nu_{as}$  (W–O<sub>b</sub>–

**Table 1** Textural and Acidity Properties of all the Catalysts

Catalyst	<i>n</i> -Butyl amine acidity (mmol/g) (Total acidity)	Surface area (m <sup>2</sup> /g)
ZrO <sub>2</sub>	0.62	170
MCM-41	0.82	659
(PW <sub>12</sub> ) <sub>3</sub> /ZrO <sub>2</sub>	1.10	146
(PW <sub>12</sub> ) <sub>3</sub> /MCM-41	1.41	360
(PW <sub>11</sub> ) <sub>3</sub> /ZrO <sub>2</sub>	0.95	226
(PW <sub>11</sub> ) <sub>3</sub> /MCM-41	1.01	253

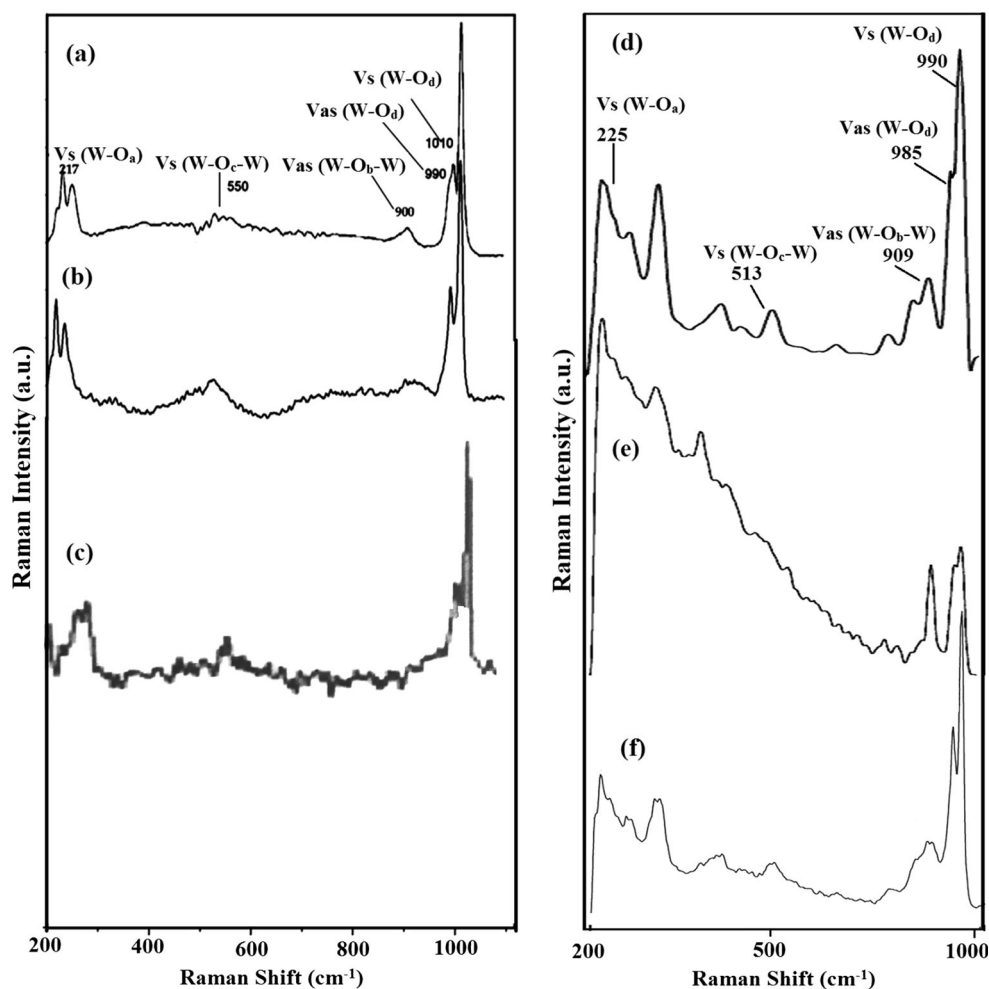
W),  $\nu_s$  (W–O<sub>c</sub>–W), and  $\nu_s$  (W–O<sub>a</sub>), respectively (Fig. 1a) where O<sub>a</sub>, O<sub>b</sub>, O<sub>c</sub>, and O<sub>d</sub> correspond to the oxygen atoms linked to phosphorus, to oxygen atoms bridging two tungsten (from two different triads for O<sub>b</sub> and from the same triad for O<sub>c</sub>), and to the terminal oxygen W=O, respectively [41]. In case of (PW<sub>12</sub>)<sub>3</sub>/MCM-41 (Fig. 1b), the absence of any significant band shifts in the spectra indicates that the environment of the Keggin unit (PW<sub>12</sub>) is retainment even after supporting to MCM-41. Raman spectra (Fig. 1c) of (PW<sub>12</sub>)<sub>3</sub>/ZrO<sub>2</sub> also shows identical

bands for PW<sub>12</sub>, which clearly indicates that PW<sub>12</sub> has been successfully incorporated on the support.

Raman spectra of PW<sub>11</sub> (Fig. 1d) show bands at 990, 985, 909, 513, and 225 cm<sup>-1</sup>, corresponding to  $\nu_s$  (W = O<sub>d</sub>),  $\nu_{as}$  (W–O<sub>d</sub>),  $\nu_{as}$  (W–O<sub>b</sub>–W),  $\nu_s$  (W–O<sub>c</sub>–W), and  $\nu_s$  (W–O<sub>a</sub>), respectively, which is identical to the reported literature [42]. The spectra of (PW<sub>11</sub>)<sub>3</sub>/MCM-41 (Fig. 1e) displays all the bands of  $\nu_{as}$  (W–O<sub>d</sub>),  $\nu_{as}$  (W–O<sub>b</sub>–W),  $\nu_s$  (W–O<sub>c</sub>–W), and  $\nu_s$  (W–O<sub>a</sub>), except  $\nu_s$  (W=O<sub>d</sub>) band. The presence of all reported bands of lacunary PW<sub>11</sub> in catalyst indicates that the Keggin structure of PW<sub>11</sub> is intact even after supporting. Raman spectra (Fig. 1f) of (PW<sub>11</sub>)<sub>3</sub>/ZrO<sub>2</sub> also shows identical bands for PW<sub>11</sub>, which clearly indicates that PW<sub>11</sub> has been successfully incorporated on the support.

The XRD patterns of the supports and catalysts are shown in Fig. 2. The XRD pattern of MCM-41 shows a sharp peak at around  $2\theta = 2^\circ$  and a few weak peaks in  $2\theta = 3^\circ$ – $5^\circ$ , which indicated a well-ordered hexagonal structure of MCM-41 (Fig. 2b). Further, the absence of characteristic peaks of crystalline phase of PW<sub>12</sub> (Fig. 2a)

**Fig. 1** Raman spectra of *a* PW<sub>12</sub>, *b* (PW<sub>12</sub>)<sub>3</sub>/MCM-41, *c* (PW<sub>12</sub>)<sub>3</sub>/ZrO<sub>2</sub>, *d* PW<sub>11</sub>, *e* (PW<sub>11</sub>)<sub>3</sub>/MCM-41 and *f* (PW<sub>11</sub>)<sub>3</sub>/ZrO<sub>2</sub>



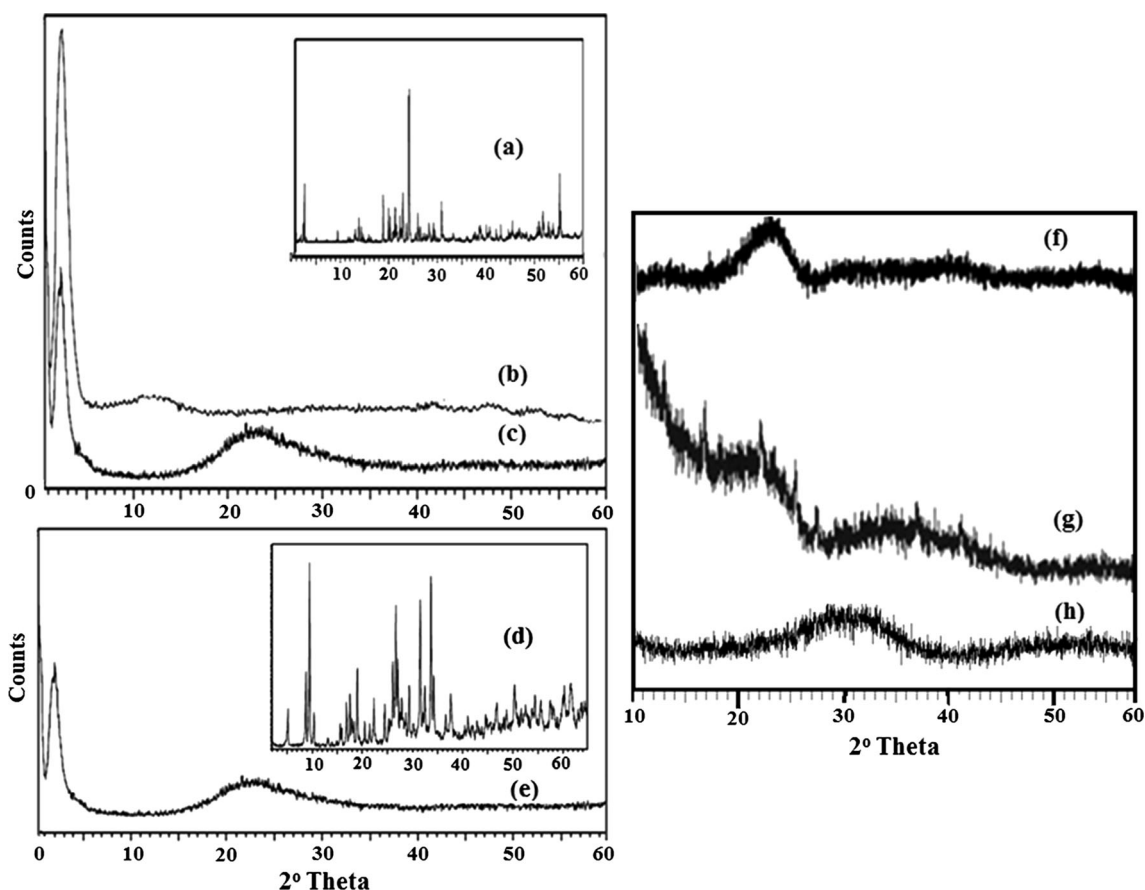


**Fig. 2** XRD pattern of *a*  $\text{PW}_{12}$ , *b* MCM-41, *c*  $(\text{PW}_{12})_3/\text{MCM-41}$ , *d*  $\text{PW}_{11}$ , *e*  $(\text{PW}_{11})_3/\text{MCM-41}$ , *f*  $\text{ZrO}_2$ , *g*  $(\text{PW}_{12})_3/\text{ZrO}_2$ , *h*  $(\text{PW}_{11})_3/\text{ZrO}_2$

indicates that  $\text{PW}_{12}$  is finely dispersed inside the hexagonal channels of MCM-41 (Fig. 2c). The large band  $2\theta = 20^\circ - 30^\circ$  (Fig. 2c, e) is characteristic of the distribution of Si–O bond lengths and is ascribed to the diffraction peak of amorphous silica, which is typical of MCM-41 material. The XRD pattern of  $(\text{PW}_{12})_3/\text{ZrO}_2$  (Fig. 2g) shows no crystalline peak corresponding to  $\text{PW}_{12}$  which indicates that  $\text{PW}_{12}$  is finely dispersed on to the surface of  $\text{ZrO}_2$ .

No separate characteristic peak of crystalline phase of  $\text{PW}_{11}$  was observed in the  $(\text{PW}_{11})_3/\text{MCM-41}$  (Fig. 2e), which indicates that  $\text{PW}_{11}$  is finely dispersed inside the hexagonal channels of MCM-41. The XRD pattern of  $(\text{PW}_{11})_3/\text{ZrO}_2$  (Fig. 2h) shows the amorphous nature of the materials indicating that the crystallinity of  $\text{PW}_{11}$  is lost on supporting it onto  $\text{ZrO}_2$ . Further, it does not show any diffraction lines of lacunary  $\text{PW}_{11}$  indicating a very high dispersion of solute as a non-crystalline form on the support surface.

FT-IR and FT-Raman spectra indicate that  $\text{PW}_{12}$  and  $\text{PW}_{11}$  are retained in the catalysts. XRD and BET studies show the uniform dispersion of  $\text{PW}_{12}$  and  $\text{PW}_{11}$  inside the channels of the support (MCM-41) as well as on the surface in case of  $\text{ZrO}_2$ .

### 3.2 Catalytic Performance

In order to examine the effects of catalyst on the direct transformation of aldehydes to corresponding esters, benzaldehyde and methanol were selected as test substrates in presence of hydrogen peroxide as oxidant (Scheme 1). The effect of different reaction variables such as benzaldehyde/ $\text{H}_2\text{O}_2$  mol ratio, amount of catalyst, reaction time and temperature were studied to optimize the conditions for maximum conversion.

To see the effect of the mole ratio, the reaction was performed by varying the mole ratio of benzaldehyde/ $\text{H}_2\text{O}_2$ , with 0.1 g of the catalyst for 6 h at  $80^\circ\text{C}$  (Fig. 3). According to the chemical dynamics, the oxidative-esterification could be improved by increasing the amount of  $\text{H}_2\text{O}_2$ . It was observed from Fig. 3 that the conversion increases with an increase in the molar ratio and reaches above 80 % for all the catalysts at mole ratio of 1:3. With a further increase in the mole ratio, there is no significant increase in conversion, however slight increase in selectivity of ester is observed.

In all the cases major selectivity of methyl ester and benzoic acid as minor product was obtained at 1:3 mol

**Scheme 1** Direct synthesis of Methyl benzoate from Benzaldehyde

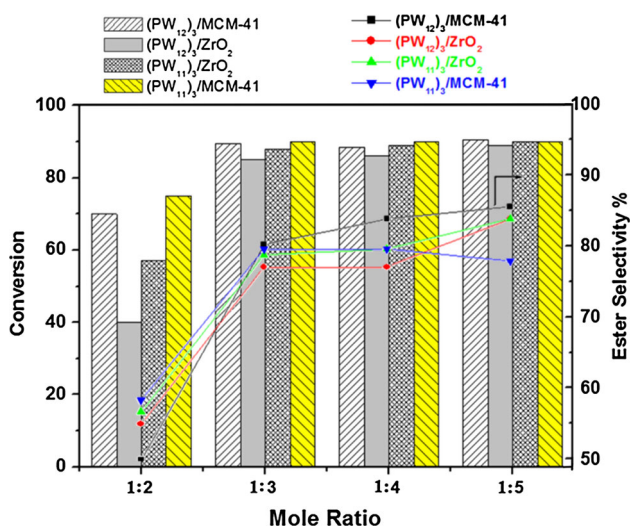
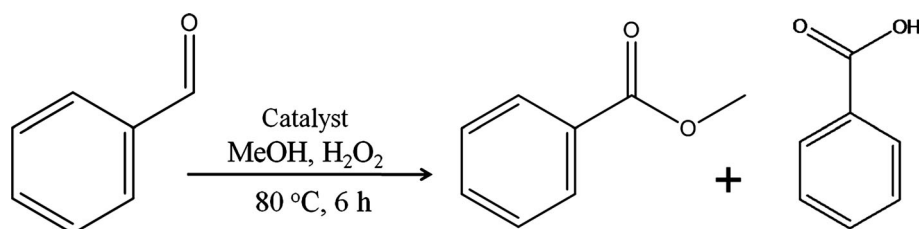


**Fig. 3** Effect of molar ratio. Reaction conditions: amount of catalyst, 100 mg; reaction temperature, 80 °C; reaction time, 6 h; methanol, 5 mL

ratio. Hence, the mole ratio of 1:3 is optimum for obtaining high conversion as well as selectivity.

The effect of the amount of catalyst on conversion was studied by varying the catalyst amount in the range of 50–200 mg. Oxidative esterification of aldehyde is significantly affected by acidity as well as oxidizing property of the catalyst. The increase in the conversion can be attributed to an increase in the number of available catalytically active sites. Hence, in the present case all the catalysts give very good conversion. It is observed from Fig. 4, that the conversion increases with an increase in the amount of catalysts and reaches a maximum of 98, 95, 90 and 95 % for (PW<sub>12</sub>)<sub>3</sub>/MCM-41, (PW<sub>12</sub>)<sub>3</sub>/ZrO<sub>2</sub>, (PW<sub>11</sub>)<sub>3</sub>/ZrO<sub>2</sub>, (PW<sub>11</sub>)<sub>3</sub>/MCM-41, at 100 mg, respectively. 100 mg of the catalyst was considered to be optimum for the maximum conversion. The selectivity to ester product increased on increasing the amount of the catalyst and major ester product was observed using 100 mg of the catalyst in relatively short reaction time (Fig. 4).

The effect of reaction time (Table 2) shows that the conversion increases with an increase in reaction time along with the selectivity toward methyl benzoate. After 6 h, no significant increase in the conversion was observed. The effect of reaction temperature (Table 2) indicates an

increase in % conversion with temperature. A maximum of 98, 95, 90, 95 % conversion was achieved respectively for (PW<sub>12</sub>)<sub>3</sub>/MCM-41, (PW<sub>12</sub>)<sub>3</sub>/ZrO<sub>2</sub>, (PW<sub>11</sub>)<sub>3</sub>/ZrO<sub>2</sub>, (PW<sub>11</sub>)<sub>3</sub>/MCM-41, at 80 °C.

It is necessary to study the effect of methanol in the reaction medium as the methanol quantity greatly affects the selectivity toward the methyl ester. Reactions were carried out by varying the methanol quantity [using (PW<sub>12</sub>)<sub>3</sub>/MCM-41] and it was observed that with increase in the methanol the selectivity to methyl benzoate increased. The selectivity of the ester was 60 % by using 2 mL of methanol as the reactant (Table 3). In contrast, 91 % of methyl benzoate (with 98 % conversion) was achieved with 4 mL of methanol. The effect of methanol was identical with all the other catalysts.

The optimum conditions are, mole ratio to benzaldehyde to H<sub>2</sub>O<sub>2</sub> = 1:3; catalyst amount 100 mg, temperature 80 °C, time 6 h, methanol 4 mL.

Under the optimised conditions, Table 4 shows that all the catalysts give conversion in the range 90–98 % as well as selectivity in the range 85–89 %. From the results it is seen that present catalytic system is not a surface type heterogeneous catalyst in which the catalytic activity is directly proportional to surface area but it is a pseudoliquid type heterogeneous catalyst in which catalytic activity is proportional to the total acidity (Table 1).

The control experiments with supports, PW<sub>12</sub> and PW<sub>11</sub> were also carried out under optimized conditions. In absence of catalyst, no ester was formed and only benzoic acid was detected. It is seen from Table 5 that the supports are not very active towards the reaction and benzoic acid was only detected as major product. Bulk PW<sub>12</sub> and PW<sub>11</sub> as catalyst showed lower activity in comparison with supported ones pointing out the importance of the concentration of surface acid sites (Table 5). In most of the runs, methyl benzoate was a main product at the end of the reaction. High TON values was obtained for active species as well as catalysts. The catalytic activity of PW<sub>12</sub> as well as PW<sub>11</sub> is retained after heterogenization on ZrO<sub>2</sub> and into the mesoporous channels of MCM-41. Thus, we were successful in synthesizing heterogeneous catalysts and overcoming the traditional problems of homogeneous catalysts.

For the rigorous proof of heterogeneity, a test [43] was carried out by filtering catalyst from the reaction mixture at

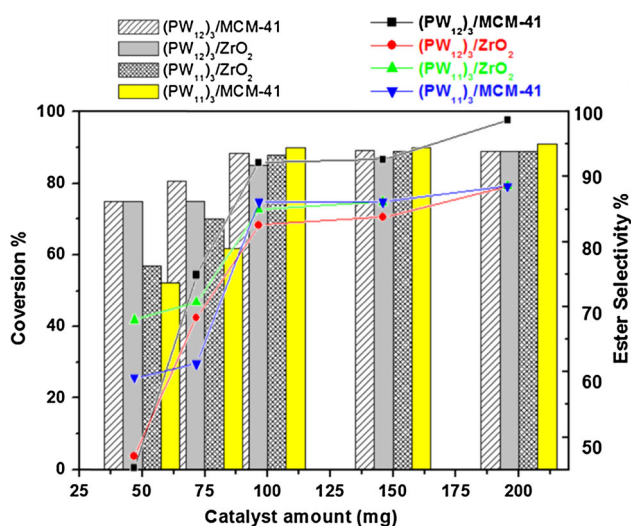


**Fig. 4** Effect of catalyst amount. Reaction conditions: mole ratio 1:3; reaction temperature, 80 °C; reaction time, 6 h; methanol, 5 mL

**Table 2** Effect of reaction temperature and time

Reaction time and temperature	% conversion <sup>a/b/c/d</sup>	% selectivity <sup>a/b/c/d</sup> methyl benzoate
2 h	50/45/60/66	30/21/40/40
4 h	88/85/95/88	90/82/85/84
6 h	98/95/95/90	91/85/89/89
8 h	98/95/95/90	92/87/89/89
60 °C	50/50/60/55	50/20/40/30
70 °C	80/87/80/77	89/50/66/60
80 °C	98/95/95/90	91/85/89/89
90 °C	98/95/95/91	80/85/90/89

<sup>a</sup> (PW<sub>12</sub>)<sub>3</sub>/MCM-41

<sup>b</sup> (PW<sub>12</sub>)<sub>3</sub>/ZrO<sub>2</sub>

<sup>c</sup> (PW<sub>11</sub>)<sub>3</sub>/MCM-41

<sup>d</sup> (PW<sub>11</sub>)<sub>3</sub>/ZrO<sub>2</sub>

80 °C after 4 h, and the filtrate was allowed to react up to the completion of the reaction (6 h). The reaction mixture of 4 h and the filtrate were analyzed by gas chromatography. No change in the % conversion or the % selectivity was found indicating the present catalyst falls into category C [43].

Any leaching of the active species from the support makes the catalyst unattractive, and hence, it is necessary to study the leaching of PW<sub>12</sub> or PW<sub>11</sub> from the support. Polyoxometalates can be quantitatively characterized by the heteropoly blue colour, which is observed when it reacts with a mild reducing agent, such as ascorbic acid. In the present study, this method was used for determining the leaching of active species from the support. One gram of

**Table 3** Effect of methanol quantity

Methanol quantity (mL)	% conversion	% selectivity	
		Methyl benzoate	Benzoic acid
1	80	30	70
2	85	60	30
3	90	85	15
4	98.5	91.5	8.5
5	99	92	8.0
6	99	93	7.0

Reaction conditions: mole ratio 1:3; reaction temperature, 80 °C; reaction time, 6 h

**Table 4** Conversion and selectivity of all the catalysts in optimized conditions

Catalysts	% conversion	% selectivity methyl benzoate	TON
(PW <sub>12</sub> ) <sub>3</sub> /MCM-41	98	91	1,224
(PW <sub>12</sub> ) <sub>3</sub> /ZrO <sub>2</sub>	95	85	1,186
(PW <sub>11</sub> ) <sub>3</sub> /MCM-41	95	89	1,179
(PW <sub>11</sub> ) <sub>3</sub> /ZrO <sub>2</sub>	90	89	1,166

Reaction conditions: mole ratio 1:3; catalyst amount 100 mg, reaction temperature, 80 °C; reaction time, 6 h; methanol, 4 mL. Turnover number (TON) = moles of product obtained/moles of catalyst (active species)

catalyst with 10 mL of conductive water was refluxed for 24 h. Then, 1 mL of the supernatant solution was treated with 10 % ascorbic acid. Development of blue colour was not observed, indicating that there was no leaching. The same procedure was repeated with alcohols and the filtrate of the reaction mixture after completion of the reaction in order to check the presence of any leached PW<sub>12</sub> or PW<sub>11</sub>. The absence of blue colour indicates no leaching of active species from the supports.

### 3.3 Recycling of Catalysts

The catalyst was recycled to test its activity as well as stability (Table 6). The catalyst was separated from the reaction mixture by filtration, washed with methanol till the filtrate is free from the un-reacted substrate (if any), followed by washing with double distilled water and then dried at 100 °C. Catalyst from different reactions was recovered following the above procedure. The recovered catalyst was charged for the subsequent run. After each run, catalyst was collected quantitatively and the same procedure was carried out to recover the catalyst after each cycle. There was no appreciable change in % conversion using regenerated catalyst up to four cycles.

**Table 5** Control experiments

Catalysts	% conversion	% selectivity methyl benzoate	TON
MCM-41	30	–	–
ZrO <sub>2</sub>	25	–	–
PW <sub>12</sub> <sup>a</sup>	88	80	1,013
PW <sub>11</sub> <sup>a</sup>	83	75	830

Reaction conditions: mole ratio 1:3; catalyst amount

<sup>a</sup> 23 mg, reaction temperature, 80 °C; reaction time, 6 h; methanol, 4 mL

**Table 6** Recycling of the catalysts

Catalyst	% conversion			
	Fresh	1st run	2nd run	3rd run
(PW <sub>12</sub> ) <sub>3</sub> /MCM-41	98	97	96	96
(PW <sub>12</sub> ) <sub>3</sub> /ZrO <sub>2</sub>	95	93	93	92
(PW <sub>11</sub> ) <sub>3</sub> /MCM-41	95	93	93	91
(PW <sub>11</sub> ) <sub>3</sub> /ZrO <sub>2</sub>	90	88	88	87

The regenerated catalyst was characterized by FT-IR and n-butyl acidity measurements (as explained earlier) in order to confirm the retention of the catalyst structure, after the completion of the reaction as discussed earlier. The FT-IR data for the fresh as well as the regenerated catalysts are presented in Fig. 5. No appreciable shift in the FT-IR band positions of the regenerated catalysts compared to the fresh catalysts indicates the retention of structure of PW<sub>12</sub>, PW<sub>11</sub> on MCM-41 and ZrO<sub>2</sub>. Further, the acidity value for fresh (PW<sub>12</sub>)<sub>3</sub>/ZrO<sub>2</sub>, (PW<sub>12</sub>)<sub>3</sub>/MCM-41, (PW<sub>11</sub>)<sub>3</sub>/ZrO<sub>2</sub>, (PW<sub>11</sub>)<sub>3</sub>/MCM-41 (1.10, 1.41, 0.95, 1.01 mmol/g, respectively) and reused catalysts also (1.09, 1.40, 0.95, 1.01 mmol/g, respectively) did not show any appreciable change in acidity. Hence there was no deactivation of the catalyst.

### 3.4 Comparison with the Reported Catalysts

Comparison of the present catalysts with reported one is shown in Table 7. Keggin-type H<sub>3</sub>PW<sub>12</sub>O<sub>40</sub> immobilized on the surface of silica encapsulated Fe<sub>2</sub>O<sub>3</sub> nanoparticles (PW/Fe@Si) [35] showed 98 % conversion at room

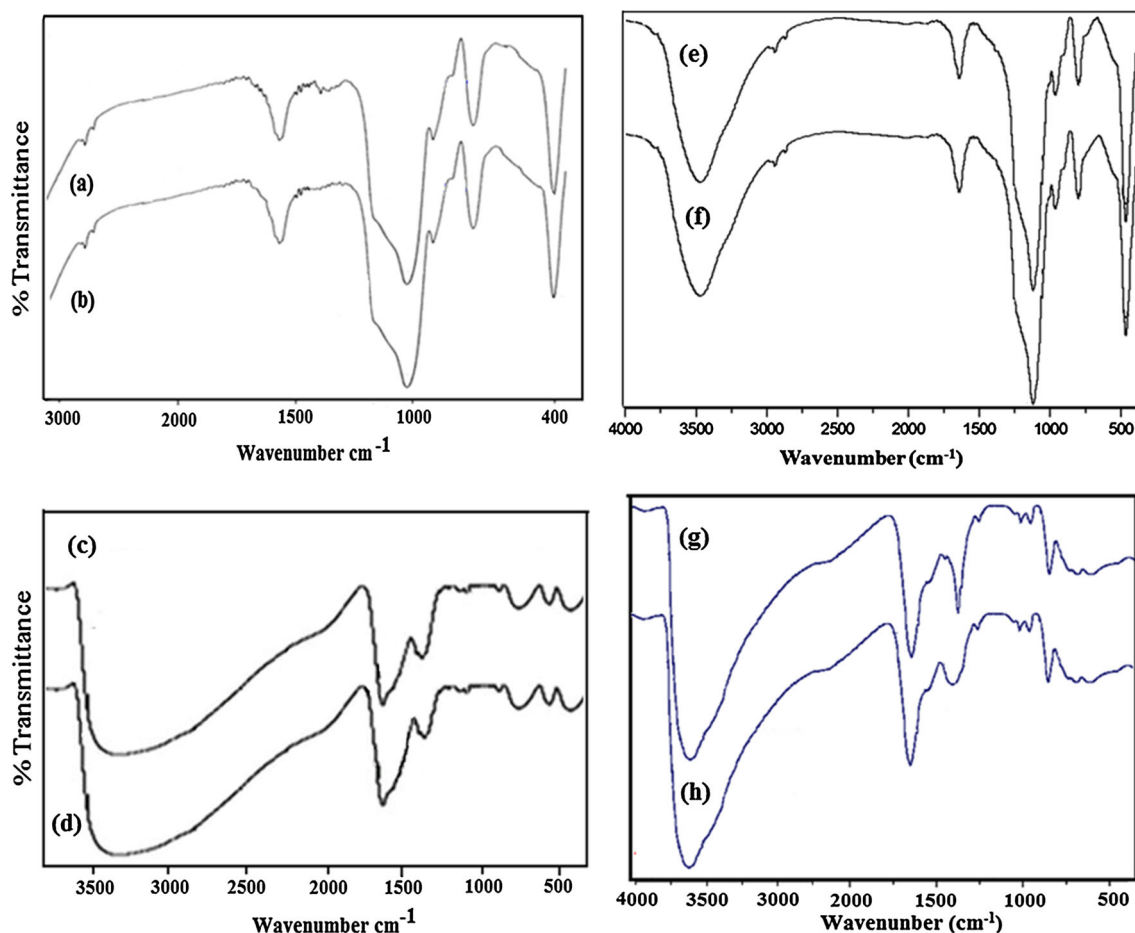


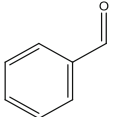
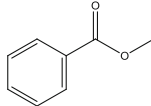
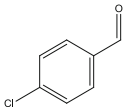
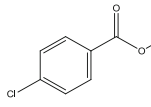
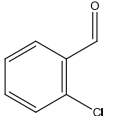
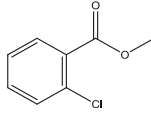
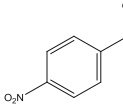
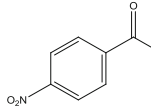
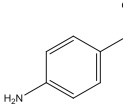
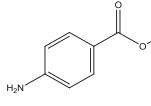
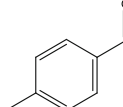
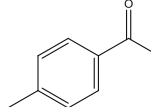
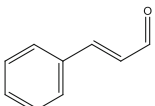
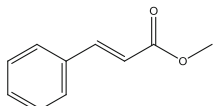
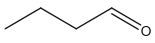
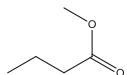
**Fig. 5** FT-IR spectra of *a* (PW<sub>12</sub>)<sub>3</sub>/MCM-41, *b* R-(PW<sub>12</sub>)<sub>3</sub>/MCM-41, *c* (PW<sub>12</sub>)<sub>3</sub>/ZrO<sub>2</sub>, *d* R-(PW<sub>12</sub>)<sub>3</sub>/ZrO<sub>2</sub>, *e* (PW<sub>11</sub>)<sub>3</sub>/MCM-41, *f* R-(PW<sub>11</sub>)<sub>3</sub>/MCM-41, *g* (PW<sub>11</sub>)<sub>3</sub>/ZrO<sub>2</sub> and *h* R-(PW<sub>11</sub>)<sub>3</sub>/ZrO<sub>2</sub>



**Table 7** Comparison of present catalysts with reported literature

Catalyst	Reaction Parameters				Conversion (%)	% selectivity for methyl benzoate	Reference
	Molar ratio	Catalyst amount (g)	T (°C)	Time (h)			
(PW <sub>12</sub> ) <sub>3</sub> /MCM-41	1:3	0.10	80	6	98	91	Present work
(PW <sub>12</sub> ) <sub>3</sub> /ZrO <sub>2</sub>	1:3	0.10	80	6	95	85	Present work
(PW <sub>11</sub> ) <sub>3</sub> /MCM-41	1:3	0.10	80	6	95	89	Present work
(PW <sub>11</sub> ) <sub>3</sub> /ZrO <sub>2</sub>	1:3	0.10	80	6	90	89	Present work
PW/Fe@Si	1:6	0.25 <sup>a</sup>	R.T	8	98	100	[35]
POM-IL	1:4	0.1	80	8	86.4	70.2	[36]
V <sub>2</sub> O <sub>5</sub> -H <sub>2</sub> O <sub>2</sub>	1:4	0.04	–	3	100	100	[44]
Pd <sub>5</sub> Pb <sub>5</sub> Mg <sub>2</sub> /Al <sub>2</sub> O <sub>3</sub>	– <sup>b</sup>	2.0	80	2	80.1	66.4	[13]
BmimBF <sub>4</sub>	– <sup>c</sup>	0.30	25	24	86	–	[14]
Cu(ClO <sub>4</sub> ) <sub>2</sub> ·6H <sub>2</sub> O, InBr <sub>3</sub>	– <sup>d</sup>	–	100	16	83	–	[45]
MnPc-APSG	1:2	0.02	60	3	100	100	[15]

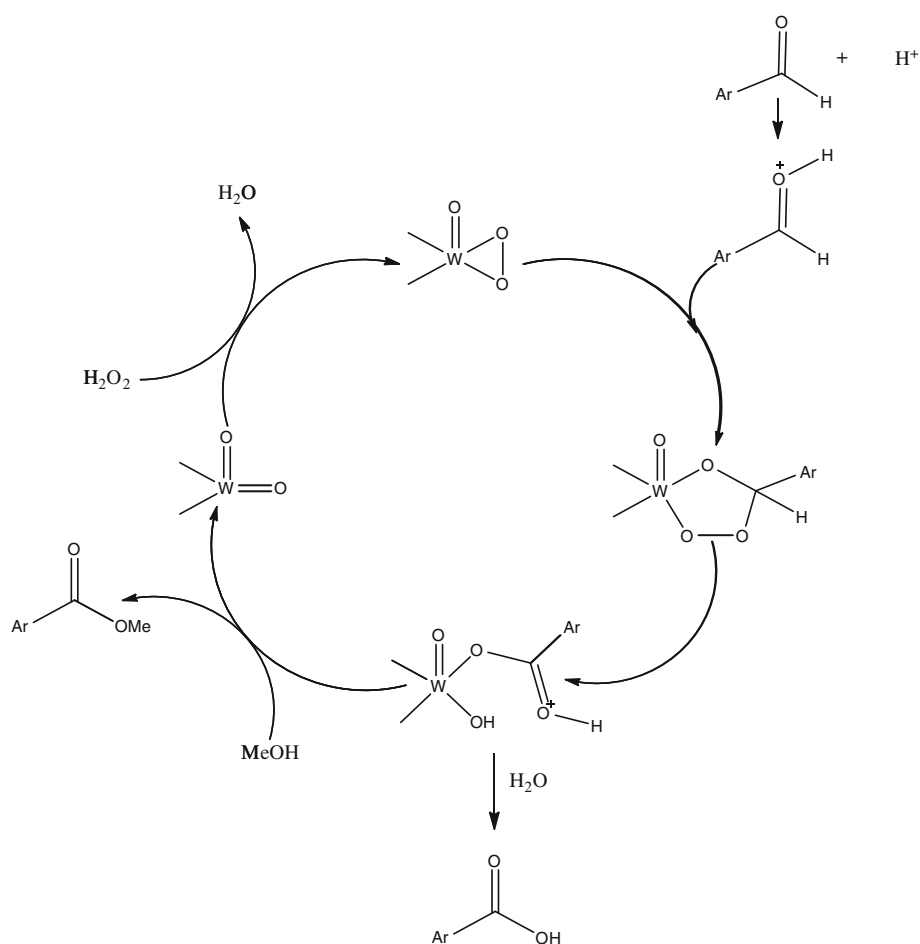
<sup>a</sup> mol%<sup>b</sup> 0.3 mol aldehyde, and 1.5 mol alcohol, O<sub>2</sub>-3 kg/cm<sup>2</sup><sup>c</sup> Reaction conditions: a mixture of 1a (0.5 mmol), oxidant agent (MnO<sub>2</sub>) and methanol was added to 0.5 mL of BmimBF<sub>4</sub> containing the base<sup>d</sup> Aldehyde (1.0 equiv), alcohol (1.5 equiv), TBHP (Oxidant), Cu(ClO<sub>4</sub>)<sub>2</sub>·6H<sub>2</sub>O (5.0 mol%), and InBr<sub>3</sub> (5.0 mol%)**Table 8** Oxidative esterification of aldehydes to corresponding esters over (PW<sub>12</sub>)<sub>3</sub>/MCM-41

Substrate	Product	% conversion	% selectivity	TON
		98	91	1,224
		82	86	1,024
		80	75	999
		78	86	949
		85	88	1,062
		87	70	1,087
		78	80	974
		76	85	949

temperature, but the molar ratio of H<sub>2</sub>O<sub>2</sub> to benzaldehyde and catalyst amount was high. H<sub>3</sub>PW<sub>12</sub>O<sub>40</sub> based Ionic liquid (POM-IL) [36] showed good conversion of 86 %

and high selectivity, but the reaction time was higher. V<sub>2</sub>O<sub>5</sub>-H<sub>2</sub>O<sub>2</sub> [44] mediated reaction yielded high ester product but the reaction required addition of HClO<sub>4</sub>.

**Scheme 2** Proposed reaction mechanism for Oxidative esterification of aldehyde with methanol



$\text{Pd}_5\text{Pb}_5\text{Mg}_2/\text{Al}_2\text{O}_3$  showed 80 % conversion with molecular oxygen as oxidant and 2.0 g catalyst in stainless steel reactor [13].

Even though high conversion was achieved, selectivity for methyl benzoate was 66.4 % and 1.0 mL 2 wt% solution of NaOH and 0.1 g  $\text{Mg}(\text{OH})_2$  were also added into the reactor to neutralize the produced carboxylic acid as an additional step. Ionic liquid BmimBF<sub>4</sub> (1-butyl-3-methylimidazolium tetrafluoroborate) [14] showed 86 % yield in 24 h, but the reaction procedure required the use of organic base and oxidant- $\text{MnO}_2$ .  $\text{Cu}(\text{ClO}_4)_2 \cdot 6\text{H}_2\text{O}$  required  $\text{InBr}_3$  for oxidative esterification of benzaldehyde using TBHP as oxidant [45], but the yield obtained was less, even though the temperature and reaction time was high. The use of Manganese phthalocyanine immobilized on silica gel (MnPc-APSG) [15] was extensively studied with high conversion (100 %) and selectivity to methyl benzoate (100 %) under mild conditions. From the extensive literature survey it was observed that reports on oxidative esterification of benzaldehyde using  $\text{H}_2\text{O}_2$  was less. In the present work all the catalysts show higher conversions under mild reaction conditions and attained good selectivity towards methyl benzoate.

### 3.5 Effect of Different Aldehyde Substrates and Proposed Reaction Mechanism

The scope of one-pot oxidative esterification was extended over different substrates of aldehyde (Table 8). The obtained results suggest that the catalyst and reaction system can withstand variety of substrates under mild reaction conditions.

In order to study the reaction mechanism, the set of reactions were carried out under two different conditions (i) in the absence of catalysts (ii) in the absence of oxidant, i.e.  $\text{H}_2\text{O}_2$ . Under both conditions, the reaction did not progress significantly, indicating that no auto-oxidation reaction takes place. From control experiments (Table 4) it was seen that support alone i.e. MCM-41 and  $\text{ZrO}_2$  did not show any significant conversion and only benzoic acid was obtained as product. From these study a tentative reaction mechanism for the present catalytic reaction is proposed in Scheme 2.

It has been reported by Chavan et al. [11] that the catalyst titanium-silicate with  $\text{H}_2\text{O}_2$  forms hydroperoxo and peroxy species which reacts with aldehyde to give titanium derived trioxolane species as intermediate. It is known for

oxidation reactions with polyoxometalates/phosphotungstate, and  $H_2O_2$  that, such reactions proceed via formation of bridging tungsten peroxo species [45–47]. In the present case, the catalysts are also expected to follow the same mechanism via the formation of an active tungsten-peroxo intermediate. In case of parent as well as lacunary phosphotungstate, same mechanism is expected. It also shows that acidity may play a role and difference in selectivity of esters for all the four catalysts might be due to the acidity of support (Table 1).

#### 4 Conclusions

Methyl esters were prepared by the clean, one-step catalytic esterification of aldehyde using  $H_2O_2$  over anchored parent as well as lacunary phosphotungstate. We have successfully achieved >90 % conversion as well as >85 % selectivity for ester. The order of activity of all the catalysts was  $(PW_{12})_3/MCM-41 > (PW_{12})_3/ZrO_2 > (PW_{11})_3/MCM-41 > (PW_{11})_3/ZrO_2$ . The advantages of present catalytic system include high substrate conversion, short reaction time, ambient temperature and TON > 1,000. The scope of one pot reaction was extended over different aldehyde substrates. The catalysts show potential of being used as a recyclable catalytic material after simple regeneration without any significant loss in the conversion. A probable reaction mechanism was proposed which suggests that acidity of the catalyst is responsible for difference in selectivity towards the corresponding esters.

**Acknowledgments** We are thankful to Department of Science and technology (DST), Project. No.SR/S5/GC-01/2009, New Delhi, for the financial support. One of the authors Ms. Sukriti Singh is thankful to the same for fellowship.

#### References

- Otera J (1993) *Chem Rev* 93:1449–1470
- Hudlicky M (1990) *Oxidations in organic Chemistry*. American Chemical society, Washington, DC
- Taft RW Jr, Newman MS, Verhoek FH (1950) *J Am Chem Soc* 72:4511–4519
- Kovi KE, Wolf C (2008) *Chem Eur J* 14:6302–6315
- Abiko A, Roberts JC, Takemasa T, Masamune S (1986) *Tetrahedron Lett* 27:4537–4540
- Connor BO, Just G (1987) *Tetrahedron Lett* 28:3235–3236
- Travis BR, Sivakumar M, Hollist GO, Borhan B (2003) *Org Lett* 5:1031–1034
- Gopinath R, Barkakaty B, Talukdar B, Patel BK (2003) *J Org Chem* 68:2944–2947
- Kiyooka SI, Ueno M, Ishii E (2005) *Tetrahedron Lett* 46:4639–4642
- Suzuki K, Yamaguchi T, Matsushita K, Iitsuka C, Miura J, Akaogi T, Ishida H (2013) *ACS Catal* 3:1845–1849
- Chavan SP, Dantale SW, Govande CA, Venkatraman MS, Praveen C (2002) *Synlett* 2:267–268
- Marsden C, Taarning E, Hansen D, Johansen L, Klitgaard SK, Egeblad K, Christensen CH (2008) *Green Chem* 10:168–170
- Diaoa Y, Yana R, Zhanga S, Yanga P, Li Z, Wanga L, Donga H (2009) *J Mol Catal A* 303:35–42
- Chiarotto I, Feroci M, Sotgiu G, Inesi A (2013) *Tetrahedron* 69:8088–8095
- Sharma RK, Gulati S (2012) *J Mol Catal A* 363–364:291–303
- Caliman E, Dias JA, Dias SCL, Prado AGS (2005) *Catal Today* 107–108:816–825
- Sawant DP, Vinu A, Jacob NE, Lefebvre F, Halligudi SB (2005) *J Catal* 235:341–352
- Khdera AERS, Hassana HMA, El-Shall MS (2012) *Appl Catal A* 411–412:77–86
- Braga PRS, Costa AA, de Freitas EF, Rocha RO, de Macedo JL, Araujo AS, Dias JA, Dias SCL (2012) *J Mol Catal A* 358:99–105
- Bi L, Dickman M, Kortz U, Dix I (2005) *Chem Commun* 3962–3964
- Pope MT (2004) *Comprehensive Coordination Chemistry. II: From Biology to Nanotechnology*, ed. A. G. Wedd, Vol 4 Elsevier, Oxford p. 635–678
- Yamase T, Pope MT (2002) *Polyoxometalate chemistry for nanocomposite design*. Kluwer, New York
- Hill CL (1998) *Chem Rev* 98:1–2
- Kozhevnikov IV (1998) *Chem Rev* 98:171–198
- Mizuno N, Misono M (1998) *Chem Rev* 98:199–218
- Dupont P, Lefebvre F (1996) *J Mol Catal A* 114:209–213
- Okuhara T (2002) *Chem Rev* 102:3641–3666
- Massart R, Contant R, Fruchart JM, Clabrini JP, Fournier M (1977) *Inorg Chem* 16:2916–2921
- Brahmkhatri V, Patel A (2011) *Appl Catal A* 403:161–172
- Patel A, Singh S (2014) *Fuel* 118:358–364
- Shringarpure P, Patel A (2008) *Dalton Trans* 30:3953–3955
- Shringarpure P, Patel A (2010) *Dalton Trans* 29:2615–2621
- Shringarpure P, Patel A (2011) *Chem Eng J* 173:612–619
- Patel A, Singh S (2013) *Ind Eng Chem Res* 52:10896–10904
- Rafiee E, Eavani S (2013) *J Mol Catal A* 373:30–37
- Li H, Qiao Y, Hua L, Hou Z, Feng B, Pan Z, Hu Y, Wang X, Zhao X, Yu Y (2010) *Chem Cat Chem* 2:1165–1170
- Brahmkhatri V, Patel A (2011) *Ind Eng Chem Res* 50:6620–6628
- Patel S, Purohit N, Patel A (2003) *J Mol Catal A* 192:195–202
- Sahu HR, Rao GR (2000) *Bull Mater Sci* 23:349–354
- Okuhara T, Mizuno N, Misono M (1996) *Adv Catal* 41:133–252
- Deltcheff CR, Fournier M, Franck R, Thouvenot R (1983) *Inorg Chem* 22:207–216
- Li B, Ma W, Liu J, Zuo S, Li X (2012) *J Colloid Interface Sci* 362:42–49
- Sheldon RA, Walau M, Arends IWEC, Schuchardt U (1998) *Acc Chem Res* 31:485–493
- Gopinath R, Patel BK (2000) *Org Lett* 2:577–579
- Yoo WJ, Li CJ (2007) *Tetrahedron Lett* 48:1033–1035
- Mizuno N (2008) *Mechanisms in homogeneous and heterogeneous epoxidation catalysts*. S. Ted Oyama (ed), chap 4. Elsevier, New York
- Dengel A. C, Griffith VVP, Parkin BC (1993) *J Chem Soc Dalton Trans* 2683–2688